Journal of Applied Sciences

ISSN 1812-5654

science alert

ANSInet
an open access publisher
http://ansinet.com

Journal of Applied Sciences 11 (6): 962-970, 2011
ISSN 1812-5654 / DOI: 10.3923/jas.2011.962.970

Numerical Simulation of Unsteady Flow to Show Self-starting of Vertical Axis Wind Turbine Using Fluent

Habtamu Beri and Yingxue Yao
Department of Manufacturing and Automation, Harbin Institute of Technology,
Harbin, 150001, China

Abstract: The study of this paper is to show the effect of modified airfoil at the trailing edge on self starting of vertical axis wind turbine at low tip speed ratios using computational fluid dynamic analysis. A moving mesh technique was used to investigate two dimensional unsteady flow around Vertical Axis Wind Turbine (VAWT) model using fluent solving Reynolds average Navier-strokes equation. The model was created with airfoil modified from conventional NACA0018 to be flexible at 15° from the main blade axis at the trailing edge located about 70% of the blade chord length. Unsteady numerical simulations of the model were then conducted at low tip speed ratios, 0.1, 0.25, 0.75 and 1. The steady state performance of the model was also conducted at three different orientations of the airfoils using different wind speeds. The Simulation results were then compared to cambered airfoil NACA2415 which is self starting. The Simulation result shows that the modified airfoil has shown better self- starting performance both in unsteady and steady flow condition for the modeled turbine.

Key words: Wind turbine, vertical axis, moving mesh, wind energy, mesh, unsteady flow, simulation

INTRODUCTION

For centuries, mankind has harnessed the power of wind to sail ships and drive wind mills to grind grain. The earliest-known design is the vertical axis system developed in Persia about 500-900 A.D and the first known documented design is also of a Persian windmill, which had a shield to block the wind from the half of the rotor moving upwind (Erich, 2006). It is widely believed that vertical axis windmills have existed in China for 2000 years, however the earliest documentation of a Chinese windmill was in 1219 A.D. by the Chinese statesman Yehlu Chhu-Tshai. Here also, the primary applications were apparently grain grinding and water pumping. The modern VAWT was first patented in France (1925) and in the U.S. (1931) by Georges Jean-Marie Darrieus (Darrieus, 1931).

Wind energy became significant in the energy crises experienced in the early 1970s to generate electrical energy instead of mechanical energy and currently there are two categories of modern wind turbines, namely Horizontal Axis Wind Turbines (HAWT) and Vertical Axis Wind Turbines (VAWT) (Izli *et al*., 2007). VAWT is classified into two categories:

- Savonious type VAWT
- Darrieus type VAWT

The Savonius-type VAWT was invented by a Finnish engineer S.J. Savonius in 1922 (Savonius, 1931). The speed of the Savonius wind turbine cannot rotate faster than the speed of the wind and so they have a Tip Speed Ratio (TSR) of 1 or below. The working principle of Savonius wind turbine is shown in Fig. 1.

Darrieus VAWTs are mainly of two types, namely Eggbeater Darrieus rotor and H-Darrieus or simply H- rotor. It was first patented in France (1925) and in the U.S. (1931) by Georges Jean-Marie Darrieus which included both the Eggbeater Curved Bladed) and Straight-bladed VAWTs. His idea received little attention and in the late 1960s, the design was independently re-invented by Canadian researchers' South and Rangi at the National Research Council in Ottawa (South and Rangi, 1973). Figure 2 shows the concept of the two types of Darrieus type vertical axis wind turbine.

A Darrieus wind turbine can spin at many times the speed of the wind hitting it (i.e., the Tip Speed Ratio (TSR) is greater than 1). Hence, a Darrieus wind turbine generates less torque than a Savonius but it rotates much faster.

Early developments in the 1970-80s demonstrated that though the VAWT are slightly less efficient than their HAWT counterpart, they have some clear advantages (Islam *et al*., 2005). The main difference between VAWTs and HAWTs is that the VAWT's ability

Corresponding Author: Habtamu Beri, Department of Manufacturing and Automation, Harbin Institute of Technology, Harbin, 150001, No. 92 Da-zhi Street, Zhizao building P.O.B 422, China
Tel: 0451-86403218 Fax: 0451-86413810

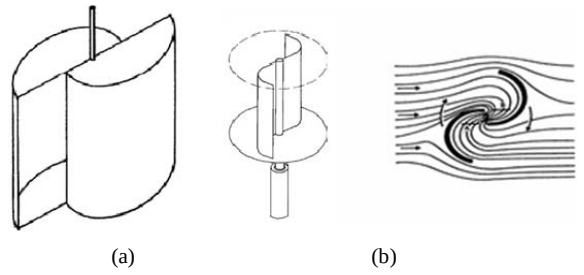

(a) (b)

Fig. 1: (a) Concept of Savonius VAWT (b) Savonius VAWT and air flow

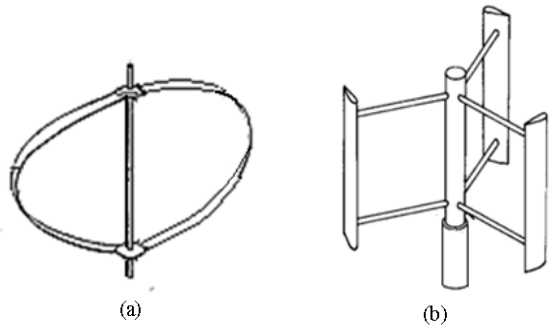

(a) (b)

Fig. 2: (a) concept of curved blade (eggbeater (b) concept of three bladed H-rotor

to accept wind from any direction, i.e., it is omni-directional. This has several advantages. The turbine does not require a yaw system, which is costly and could fail during operation. The yaw system includes both a control system and a drive mechanism. The costs associated with such a system include the cost of the equipment itself, installation cost and costs for operation and maintenance. Furthermore, with an omni-directional turbine there are no power losses during the time it takes for the turbine to yaw or during short wind gusts with temporary changes in wind direction (Roynarin *et al*., 2002).

An omni-directional turbine can be situated at places where the wind is turbulent and where the wind direction changes often. For this reason, VAWTs have an advantage over HAWTs in high mountain areas, in regions with extremely strong or gusty winds and in urban areas. Furthermore, the VAWT is less noisy than the HAWT, which becomes even more important in urban areas (Riegler, 2003). Investigations indicate a clear advantage in using VAWTs at rooftops (Mertens, 2003).

Blades of VAWT may be of uniform section and untwisted, making them relatively easy to fabricate or extrude, unlike the blades of HAWT, which should be twisted and tapered for optimum performance. Furthermore, almost all of the components requiring maintenance are located at the ground level facilitating the maintenance work appreciably (Islam *et al*., 2005). However, its high torque fluctuations with each revolution, no self-starting capability are the drawbacks (Kirke, 1998; The worlds of David Darling, 2009).

The majority of research on VAWT design was carried out during the late 1970s and early 1980s, notably at the USA Department of Energy Sandia National Laboratories (Dodd, 1990) and in the UK by Reading University and VAWT Ltd, who erected several prototypes including a 500 kW version at Carmarthen Bay (Price, 2006). When it became accepted that HAWTs were more efficient at these large scales, interest was lost in VAWT designs and HAWTs have since dominated wind turbine designs. Due to this, very little research can be found in the last couple of decades on the VAWT.

It is common to find on various literature and commonly believed that VAWTs are less efficient than the commonly known HAWTs. However, as some literature shows, that does not really indicate the truth. VAWT technology is not widely commercialized, not because of it has been shown to be inferior to HAWT technology. Rather, it appears to be because the VAWT technology is much different from HAWT technology and relatively few companies have made the investment required to truly understand and objectively evaluate the VAWT (Berg, 1996). VAWTs could develop similarly as HAWTs if money and time was invested in research (Eriksson *et al*., 2008).

According to Kirke (1998) majority of the previously conducted research activities on VAWT focused on straight bladed VAWTs that equipped with symmetric airfoils like NACA0012, NACA0015 and NACA0018 profiles which were unable to self-start. Due to the cyclical variation in angle of attack, blades are stalled and generate low or negative (i.e. reverse) torque for most azimuth angles at low tip speed ratio. To solve this problem, numerous attempts were made to improve self staring of VAWT by different scholars including (Lazauskas, 1992; Dereng, 1981; Barker, 1983; Hurley, 1979; Wakui *et al*., 2005; Drees, 1979; Liljegren, 1984) and others. Though the approaches were tend to contribute in the increases of starting torque, reductions in peak efficiencies and working on the operating range were some of the major problems.

These days, there is revival of interests regarding VAWTs as several universities and research institutions have carried out extensive research activities and developed numerous designs based on several aerodynamic computational models (Islam *et al*., 2008). A comparative study made by Eriksson *et al*. (2008) cited

above shows that VAWTs are advantageous to HAWTs in several aspects. Other many research works showed that VAWT has the potential to compete with the more widely used conventional HAWTs if the inability of the turbine to self-start is resolved.

The present paper attempts to show self-starting capability of darrieus type VAWT by modifying the conventional symmetrical airfoil which is not self starting itself. NACA0018 airfoil was made to be divided into two parts at about 70% of the chord length as shown in Fig. 3. The trailing edge inclined at 15° from the main blade axis was modeled in gambit modeling software. The model created was then read into commercial CFD software, Fluent 6.3.26 version for computational analysis of the two dimensional (2D) unsteady flow around the turbine. 2D unsteady flow analysis for the modeled airfoil section VAWT was analyzed based on Reynolds Averaged Navier-stokes (RANS) equation using moving mesh technique.

The basic idea for the modification of the airfoil was to make use of high lift forces for self -staring capability. As the velocity of the wind that passes on the top surface is greater than the velocity of the wind on the lower surface of the modified airfoil, high pressure difference that contribute to self starting of the turbine assumed to be created at low tip speed ratio. Then the trailing edge can be allowed to take the same axis orientation as the main airfoil for the operation of the turbine at higher tip speed ratios.

MATERIALS AND METHODS

Computational fluid dynamic, CFD tool solving the Reynolds-averaged navier-stroke equations based on moving mesh technique was conducted on October 8, 9 and 10, 2010 using high speed processor computer. The laboratory is located in the zoo campus of Harbin Institute of Technology, Department of Manufacturing and Automation. The analysis incorporates 2D unsteady flow of vertical axis wind turbine model with NACA0018 modified airfoil blade section at different tip speed ratios and steady flow conditions at three different orientations of the airfoils. The procedures followed in the analysis are as follows.

Computational analysis: The basic structure of the vertical axis wind turbine selected for the computational analysis is as shown in Fig. 4. It is a fixed pitch type with three straight blades of modified airfoil. The basic analysis system of the turbine is shown in Fig. 5.

As the blades turn about the central shaft, they encounter an incident wind that is composed of the

Fig. 3: Modified geometry of NACA0018 airfoil

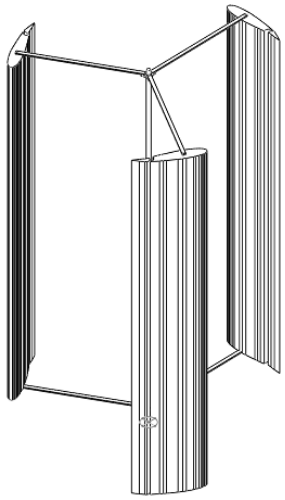

Fig. 4: Schematic representation of VAWT model created with solid works

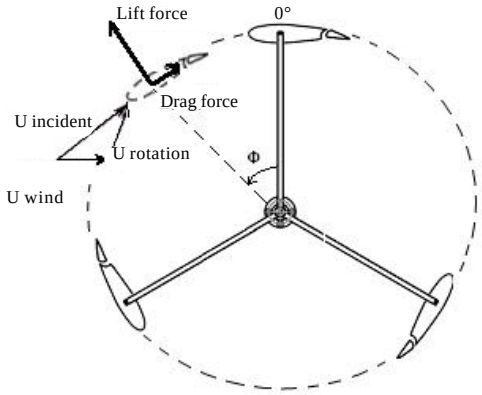

Fig. 5: Topographic view of the model with lift and drag component

ambient local wind velocity and the blade rotational velocity as indicated in Fig. 5. This incident wind velocity generates lift and drag forces on the blades, which can be decomposed into a thrust force and a radial force on the turbine arms.

- **Note:** Lift is defined as the force perpendicular to incident wind velocity and drag is defined as the force parallel to the incident wind velocity

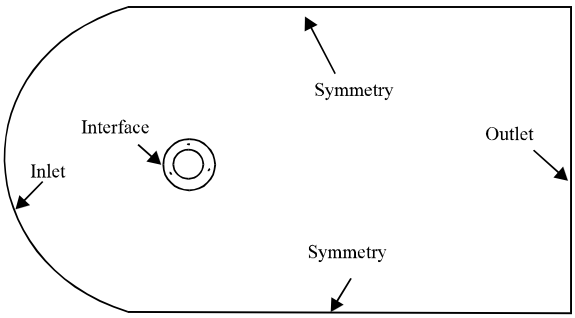

Fig. 6: Boundary conditions

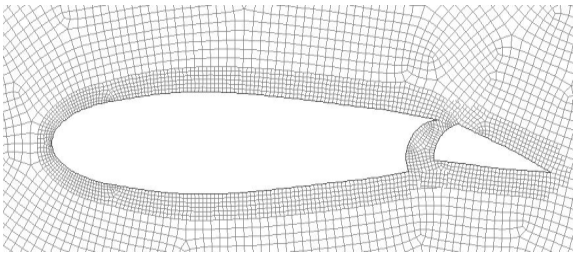

Fig. 7: Mesh near airfoil

Computational domain: The modified NACA0018 airfoil was used for the analysis of 2D unsteady flow. The airfoil was set to 0.2 m chord length and the turbine radius was set to 2 m. Gambit 2.3.16 version modeling software was used to create 2D model and to generate mesh. The domain size was created with a rotating sub-domain surrounding the blades and stationary sub domains in the remaining region. Mesh for the rotating sub-domain, central stationary sub-domains and stationary sub domain located to the right side of rotating sub-domain were generated with square pave. Frontal stationary sub-domain and the last stationary sub-domain located at far end of the outlet are generated with structured type of grid. The rotating sub-domain was set to a major diameter of 5 m and minor 3 m. The inlet width and out let width were set to 3 times the major diameter of rotating sub-domain. The inlet was located 3 times the major diameter of rotating sub-domain upstream and outlet 6 times the major diameter of the rotating sub-domain downstream.

Computational method: The model and mesh generated in gambit modeling software were read into the commercial CFD code, fluent V.6.2.30 for numerical iterative solution. The RANS equations were solved using the green-gauss cell based gradient option and the sliding mesh method was used to rotate the sub-domain for the turbine blades. For pressure-velocity coupling, the simple algorithm was

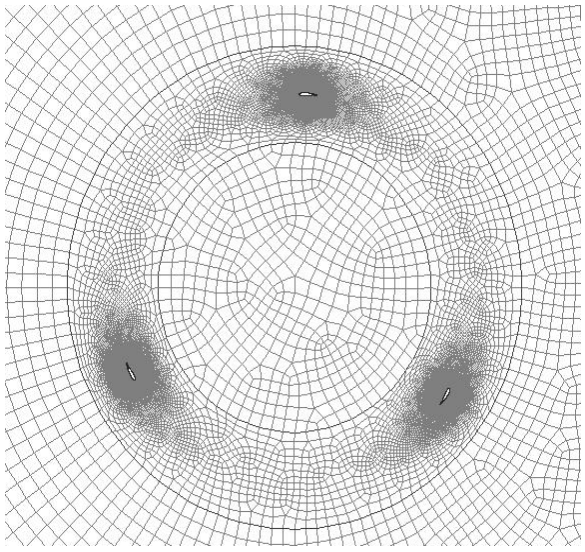

Fig. 8: Rotating sub-domain

used. Standard was set as pressure discretization and first order upwind was set for momentum. Time integration was done implicitly and the minimum convergence criteria were set to 1e-06. The RNG k-epsilon model was adapted for the turbulence closure.

For the moving mesh simulations, the computational sub-domain is split into a moving part around the turbine and a fixed part for the fixed environment. The rotational motion is simulated by allowing the mesh block around the wind turbine to rotate at constant angular velocity. The mesh movement is defined explicitly by specifying time-varying positions for all of the moving mesh block cell vertices. An interface boundary surrounding the moving mesh part within the model slides at the specified velocity. This represents the relative motion between the rotating wind turbine and the fixed environment.

Boundary conditions: The boundary conditions are shown in Fig. 6. The inlet was defined as a velocity inlet, which has constant inflow velocity while the outlet was set as a pressure out let, keeping the pressure constant. The velocity at the out let was determined by the extrapolation from inside. The no slip shear condition was applied on the turbine blades, which sets the relative velocity of blades to zero. There were four domains in the computational domain with 522 cells around each blade. The cells were concentrated near the blades as shown in Fig. 7 for better result.

The flow condition used for the analysis is shown in Table 1. Time step size was set corresponding to 2 degree for each rotational speed of the rotor (ω) given

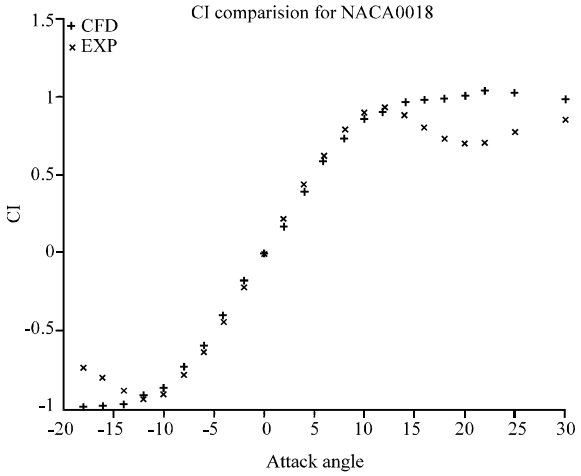

Fig. 9: Lift coefficient comparison, for Re=360,000

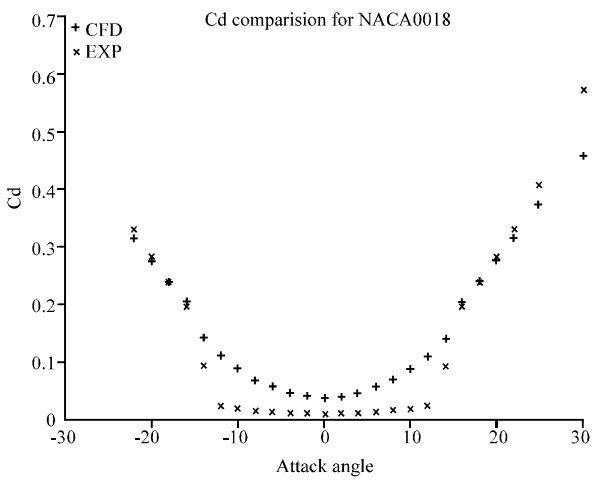

Fig. 10: Drag coefficient comparison, for Re=360,000

Table 1: Flow conditions

TSR (λ)	Velocity ms^{-1}	Turbine ang.vel. ($rad\ s^{-1}$)	Time step size(s)
0.1	6	0.3	0.116347
0.25	6	0.75	0.046539
0.5	6	1.5	0.023269
0.75	6	2.25	0.015513
1	6	3	0.011635

in Table 1 corresponding to each TSR. One hundred and twenty iterations were used per time step.

The operating speed of the turbine, expressed as tip speed ration (TSR) was set between 0.1 and 1.

- **Note:** TSR(λ) is defined as:

$$TSR = \frac{R\omega}{V\infty} \quad (1)$$

where, R is the turbine radius, ω is angular velocity and V∞ is the free stream velocity

Code verification: To verify the reliability of the computational method, hydrodynamic forces acting on the conventional symmetrical airfoil, NACA0018 was computed from different angles of attack. The cord length was set to 1m and the corresponding cord -based Reynolds number Re, was 360,000. The converged solution was obtained after 1500 iterations. Figure 9 shows the comparison of the computational solutions and experimental data (Sheldahl and Klimas, 1981). The computed lift forces are in good agreement with the experimental data for angles of attack between -10 and 10 degree which is considered to be the normal operating range of turbine blades. The drag coefficient comparison is also shown in Fig. 10.

RESULTS

Figure 11 shows simulated torque values for the modeled NACA0018 modified airfoil at lower TSR. It shows the torque values at different azimuth angle in N-m for complete revolution of TSRs 0.1, 0.25, 0.5, 0.75 and 1. The torque values were obtained from coefficient moment (Cm) of the modeled airfoil, air density, turbine area, free stream velocity chosen and the radius of the turbine modeled. The graph shows that the average torque values at each of the TSR simulated are positive.

Figure 12 shows simulated torque values for NACA2415 cambered airfoil modeled in the same way as the modified NACA0018 using the same parameter for comparison. It shows the torque at different azimuth angles in N-m for complete revolution of TSRs 0.1, 0.25, 0.5, 0.75 and 1. The torque values were obtained using the same principle as mentioned above. As can be seen from the graph, the torque values are higher for the modified airfoil compared to the camber airfoil.

Figure 13 shows the coefficient of moment (Cm) of the simulated model for NACA0018 and NACA2415. This coefficient determines the average torque of wind turbines. The Cm values were obtained from the average moment of the three airfoils modeled through CFD computational analysis. As can be seen, Cm near zero is higher and seems to reduce up to TSR = 0.5 and then starts to rise. It is also clear that the Cm of modified NACA0018 is greater than that of NACA2415 camber airfoil.

Figure 14 shows the Coefficient of Power (Cp) for the modified NACA0018 airfoil. The graph is generated by combining the performance of turbine trailing edge inclined modeled for TSR 0.1 to 1 and without inclination

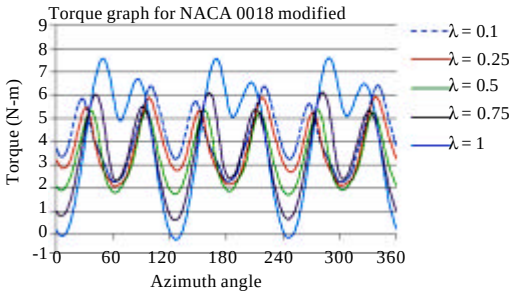

Fig. 11: Torque for modified NACA0018

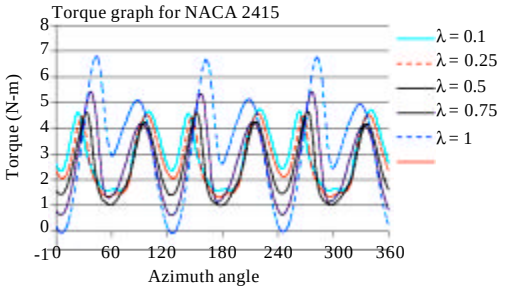

Fig. 12: Torque for NACA2415 camber airfoil

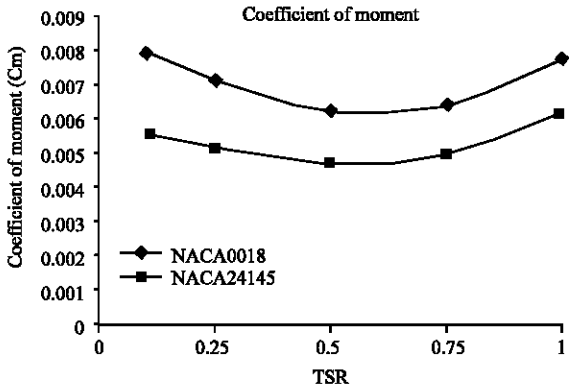

Fig. 13: Comparison of Cm for NACA2415 and NACA0018 modified airfoil

of the trailing edge for TSR greater than 1. The Cp was obtained from the ratio of the modeled turbine power to the available wind power in the air and used to determine the performance of the turbines.

Figure 15 shows the steady state torque values at TSR 0 for different wind speeds at three different orientations of the blades. The blade orientations were taken at three different azimuth angles of 0, 45 and 90° as shown in Fig. 16. This helps to show the performance of the turbine at its steady state. The simulation result shows that the torque values are positive at all the orientations and increases with increase of wind velocity.

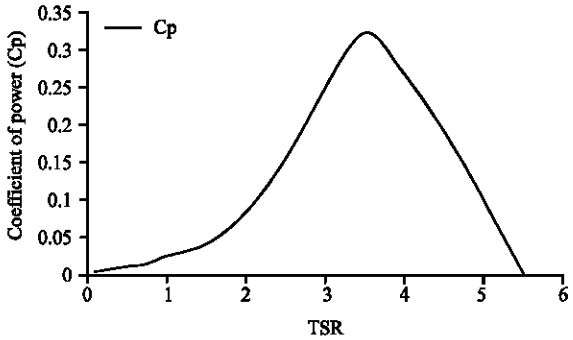

Fig. 14: Cp Curve of the modified airfoil

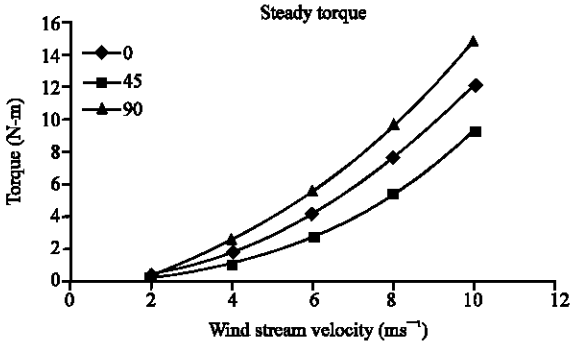

Fig. 15: Torque versus velocity at three locations of blades

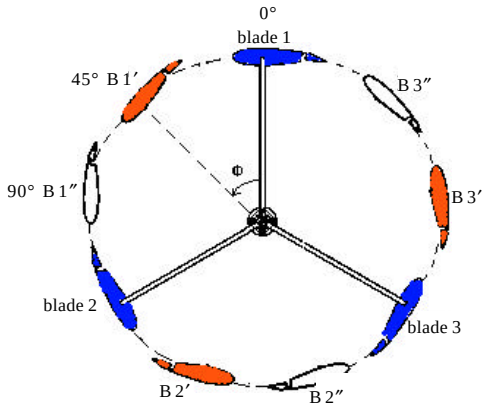

Fig. 16: Blades orientation at different azimuth angle

With this result it is possible to conclude that the turbine can self start from steady state at any orientation of the blades.

In Fig 16, Blade 1, 2 and 3 represent the steady state orientation of the turbine at azimuth angle of 0°. B1', B2', and B3', represent the orientation of the turbine at azimuth angle of 45°. Lastly B1, B2 and B3" represent the third steady state orientation of the turbine at azimuth angle of 90°.

DISCUSSION

Blade aerodynamic forces and torque are computed from the solution of RANS equations through the integration of the pressure and shear stress over the blade surface. The total wind turbine force components and torque are obtained by adding the 3 blade force components and torque. The driving torque is obtained by calculating the average of the instantaneous values corresponding to the last revolution of the rotor. These values were used to derive the expected wind turbine power coefficient (Cp). The turbine was allowed to turn until stable torque was created and the minimum number of turns used for this model was 6 turns.

Power of the turbine is defined as:

$$P = \omega T \quad (2)$$

where, p is expected output power of turbine, ω is angular velocity of turbine, T averaged torque

Cp is then calculated as:

$$Cp = \frac{P}{0.5*\rho*A*V^3\infty} \quad (3)$$

where, ρ is the air density, V∞ free stream velocity, A frontal area of the turbine

Symmetrical airfoils NACA0012, NACA0015 and NACA0018 are the conventional airfoil sections used in Darrieus type VAWTs. However, the main drawbacks with these types of sections are their minimum or negative torque generation at lower TSRs. For comparison of the modified airfoil result, NACA 2415 camber airfoil was numerically analyzed with computational fluid dynamic analysis taking the same parameter as the modified airfoil. The simulation result is in agreement with previous works (Lazauskas, 1992; Barker, 1983; Kirke and Lazauskas, 1991; Healy, 1978; Kotb, 1990; Habtamu and Yingxue, 2011) that camber airfoil can increase staring torque but reduction in peak efficiency and operating in narrower ranges are the draw backs.

The self- starting capability of the modified airfoil is then compared to the cambered airfoil as shown in Fig. 13. As can be seen from the simulation result, the modified airfoil has shown a better coefficient of moment for the simulated model than the camber airfoil. This indicates that the turbine can accelerate at lower TSR which cannot be possible using symmetrical airfoils.

The steady state result shown in Fig. 15 at TSR 0 also indicates that the modeled turbine can generate positive torques at all the selected three orientations. This indicates that the turbine can start to turn from stationary point. The coefficient of moment and the steady result implies that the modified airfoil has shown good self-starting for the modeled turbine at low tip speed ratios.

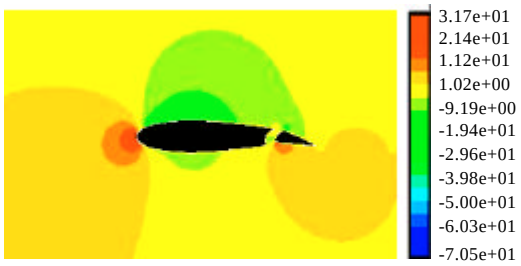

Fig. 17: Static pressure contour at 0° angle of attack in Pascal

Fig. 18: Static pressure contour at 10° angle of attack in Pascal

Fig. 19: Static pressure contour at 16° angle of attack in Pascal

Figure 17 to 19 shows the static pressure distribution around the airfoil in Pascal for angle of attacks 0, 10 and 16 degrees, respectively. Depending on the color of the static pressure contour, one can predict where the pressure is high and lower around the airfoil using the value of pressure displayed on the status bar for the modeled airfoil. Referring back the relationship between pressure and velocity from the Bernoulli equation one can also able to predict where the flow velocity of the wind high and low around the airfoil.

The present work has attempted to analyze the performance of Darrieus type VAWT with three fixed straight blades from different perspective through modification of existing airfoil at low tip speed ratios. The research is aimed to contribute to the current literature in renewable energy and self staring studies of vertical axis wind turbine which is a promising design for diversified applications.

CONCLUSIONS

2D unsteady flow of VAWT with NACA0018 modified geometry blade section based on fixed pitch three blades was analyzed using computational fluid dynamics. The model was analyzed at lower TSRs 0.1, 0.25, 0.5, 0.75 and 1. The model was also analyzed for its performance at its steady state or TSR = 0. The coefficients of moments were then compared with NACA2415 camber airfoil which is self- starting that is analyzed using the same parameter. Coefficients of moments for the higher torque were also analyzed without the inclination of the trailing edge for performance prediction. The simulation result shows that the modified airfoil has shown better performance in self- staring of the turbine at lower TSRs for the modeled turbine. The power coefficient of the simulated model obtained through combination is also in the normal range of turbine performance. Optimization of the airfoil through CFD is an extension of future work.

REFERENCES

Barker, J.R., 1983. Features to aid or enable self starting of fixed pitch low solidity vertical axis wind turbines. J. Wind Eng. Ind. Aerodynamics, 15: 369-380.

Berg, D.E., 1996. Vertical Axis Wind Turbines- the Current Status of an Old Technology. Sandia National Laboratories, Albuquerque.

Darrieus, G.J.M., 1931. Turbine having its rotating shaft transverse to the flow of the current. United States Patent 1835018. http://www.freepatents online. com/ 1835018.html.

Dereng, V.G., 1981. Fixed geometry self starting transverse axis wind turbine. United States Patent 4264279. http://www.freepatentsonline.com/4264279.html.

Dodd, H.M., 1990. Performance Predictions for an Intermediate-sized VAWT Based on Performance of the 34-m VAWT Test Bed. Sandia National Laboratories, Albuquerque.

Drees, H.M., 1979. Self-starting windmill energy conversion system. United States Patent 4180367. http://www.freepatentsonline.com/4180367.html.

Erich, H., 2006. Wind Turbines Fundamentals, Technologies Application, and Economics. 2nd Edn., Springer-Verlag, Berlin Heidelberg.

Eriksson, S., H. Bernhoff and M. Leijon, 2008. Evaluation of different turbine concepts for wind power. Renewable Sustainable Energy Rev., 12: 1419-1434.

Habtamu, B. and Y. Yingxue, 2011. Effect of camber airfoil on self starting of vertical axis wind turbine. J. Environ. Sci. Technol., 4: 302-312.

Healy, J.V., 1978. The influence of blade camber on the output of vertical axis wind turbines. Wind Eng., 3: 146-155.

Hurley, B., 1979. A novel vertical axis sail rotor. Proceedings of 1st Wind Energy Workshop, April 19-20, Multi-Science Publishing Co. Ltd., London, pp: 40-47.

Islam, M., D.S.K. Ting and A. Fartaj, 2008. Aerodynamic models for darrieus-type straight-bladed vertical axis wind turbines. Renewable Sustainable Energy Rev., 12: 1087-1109.

Islam, M., V. Esfahanian, D.S.K. Ting and A. Fartaj, 2005. Applications of vertical axis wind turbines for remote areas. Proceedings of 5th Iran National Energy Conference, Tehran, Iran, Spring 2005.

Izli, N., A. Vardar and F. Kurtulmu, 2007. A study on aerodynamic properties of some NACA profiles used on wind turbine blades. J. Applied Sci., 7: 426-433.

Kirke, B.K. and L. Lazauskas, 1991. Enhancing the performance of vertical axis wind turbine using a simple variable pitch system. Wind Eng., 15: 187-195.

Kirke, B.K., 1998. Evaluation of self-starting vertical axis wind turbines for stand-alone applications. Ph.D. Thesis, Griffith University, Australia

Kotb, M.A., 1990. On the use of an asymmetric profile with trailing edge extension plate for VAWT blades. Wind Eng., 14: 300-311.

Lazauskas, L., 1992. Three pitch control systems for vertical Axis wind turbines compared. Wind Eng., 16: 269-269.

Liljegren, K.L., 1984. Vertical axis wind turbine. United States Patent 4430044. http://www.freepatentsonline. com/ 4430044.html.

Mertens, S., 2003. The energy yield of roof mounted wind turbines. Wind Eng., 27: 507-518.

Price, T.J., 2006. UK large-scale wind power programme from 1970 to 1990: The carmarthen bay experiments and the musgrove vertical-axis turbines. Wind Eng., 30: 225-242.

Riegler, H., 2003. HAWT versus VAWT: Small VAWTs find a clear niche. Refocus, 4: 44-46.

Roynarin, W., P.S. Leung and P.K. Datta, 2002. The performances of a vertical Darrieus machine with modern high lift airfoils. Proceedings from IMAREST Conference MAREC 2002, Newcastle, UK.

Savonius, S.J., 1931. The S-rotor and its application. Mechanical Eng., Vol. 53,

Sheldahl, R.E. and P.C. Klimas, 1981. Aerodynamic Characteristics of Seven Airfoil Sections Through 180 Degrees Angle of Attack for Use in Aerodynamic Analysis of Vertical Axis Wind Turbines. Sandia National laboratories, Albuquerque, New Mexico.

South, P. and R.S. Rangi, 1973. The performance and economics of the vertical axis wind turbine developed at the national research council, Ottawa, Canada. Proceedings of the 1973 Annual Meeting of the Pacific Northwest Region of the American Society of Agricultural Engineers, Calgary, Alberta.

The Worlds of David Darling, 2009. The encyclopedia of alternative energy and sustainable living. http://www.daviddarling.info/encyclopedia/AEmain.html.

Wakui, T., Y. Tanzawa, T. Hashizume and T. Nagao, 2005. Hybrid configuration of Darrieus and Savonius rotors for stand-alone wind turbine-generator systems. Electrical Eng. Jap., 150: 13-22.